ADVANCED FUNCTIONAL MATERIALS
www.afm-journal.de

Development of Synthetic Platelet-Activating Hydrogel Matrices to Induce Local Hemostasis

Xiao-Hua Qin, Krystyna Labuda, Jie Chen, Veronika Hruschka, Anna Khadem, Robert Liska, Heinz Redl, and Paul Slezak*

Several hemostatic strategies rely on the use of blood components such as fibrinogen and thrombin, which suffer from high cost and short shelf-life. Here, a cost-effective synthetic biomaterial is developed for rapid local hemostasis. Instead of using thrombin, thrombin-receptor-agonist-peptide-6 (TRAP6) is covalently engineered in polyvinyl alcohol (PVA) hydrogels. Soluble PVA-TRAP6 is first prepared by covalent attachment of cysteine-containing TRAP6 onto the backbone of PVA-norbornenes (PVA-NB) through photoconjugation. Cytotoxicity studies using C2C12 myoblasts indicate that PVA-NB and PVA-TRAP6 are nontoxic. Thromboelastography reveals that hemostatic activity of TRAP6 is retained in conjugated form, which is comparable to free TRAP6 solutions with equal concentrations. A 0.1% PVA-TRAP6 solution can shorten the clotting time (CT) to ca. 45% of the physiological CT. High platelet-activating efficiency is further confirmed by platelet aggregation assay and flow cytometry (FACS). For potential clinical applications, TRAP6-presenting hydrogel particulates (PVA-TRAP6-P) are developed for local platelet activation and hemostasis. PVA-TRAP6-P is prepared by biofunctionalization of photopolymerized PVA-NB hydrogel particulates (PVA-NB-P) with TRAP6. It is demonstrated that PVA-TRAP6-P can effectively shorten the CT to ca. 50%. FACS shows that PVA-TRAP6-P can activate platelets to a comparable extent as soluble TRAP6 control. Altogether, PVA-TRAP6-P represents a promising class of biomaterials for safe hemostasis and wound healing.

1. Introduction

Uncontrolled bleeding is still the leading cause of mortality in traumatic and surgical injuries.[1] Developing effective therapeutic approaches to control bleeding is therefore of paramount clinical and social values. In the last decades, a number of hemostatic products[2] have been developed, including fibrin-based glue or sealants,[3] zeolite powders,[4] crosslinked gelatin matrix,[5] and so forth. However, each of these products has its respective limitations. Fibrin-based products suffer from high cost, short shelf-life and weak mechanical strength.[6] Zeolite minerals are prone to cause severe burns and are not degradable.[6] Crosslinked gelatin matrix could halt bleeding within minutes only when combined with high doses of thrombin.[7] Highly concentrated thrombin is known to induce apoptosis of human keratinocytes and can cause impairments in wound healing.[8] Hence, there exists a strong need to design alternative hemostatic materials with improved safety. In particular, designing an effective strategy that avoids the use of highly concentrated thrombin is a desirable solution.

Thrombin is a serine protease that plays important roles in blood clotting (coagulation).[9] As the key coagulation protease, thrombin converts soluble fibrinogen into fibrin networks with additional help of a transglutaminase (FXIII).[10] In addition, thrombin is the most potent activator of platelets by stimulating protease-activated receptors (PAR).[11,12] Upon activation by thrombin, platelets physically alter the conformation of GP IIb/IIIa receptors and provide high-affinity binding sites for fibrinogen, providing fibrinogen-crosslinked platelet aggregation. Both PAR-1 and PAR-4 are present on human platelets, yet activation of human platelets by thrombin is primarily mediated by PAR-1.[13] The molecular mechanism of PAR-1 activation by thrombin is depicted in **Scheme 1**A. PAR-1 is highly expressed in platelets,[14] and PAR-1 activation is initiated by proteolytic cleavage of part of the extracellular N-terminal domain of PAR-1 receptor by thrombin. Proteolysis generates a new N-terminal ligand domain (SFLLRN, a.k.a. thrombin receptor agonist peptide-6, TRAP6) that interacts with the receptor within the extracellular loop 2 and triggers the signaling pathway of PAR-1 activation. It has been proven that short TRAP6 peptide (SFLLRN) could work as a potent platelet activator separately and stimulates platelet aggregation via PAR-1 signaling.[15]

Dr. X.-H. Qin, K. Labuda, J. Chen, Dr. V. Hruschka, A. Khadem, Prof. H. Redl, Dr. P. Slezak
Ludwig Boltzmann Institute for Experimental and Clinical Traumatology
Austrian Cluster for Tissue Regeneration
Donaueschingenstraße 13, 1200 Vienna, Austria
E-mail: xh.qin84@gmail.com
Prof. R. Liska
Vienna University of Technology
Institute for Applied Synthetic Chemistry
Austrian Cluster for Tissue Regeneration
Getreidemarkt 9, 1060 Vienna, Austria

DOI: 10.1002/adfm.201501637

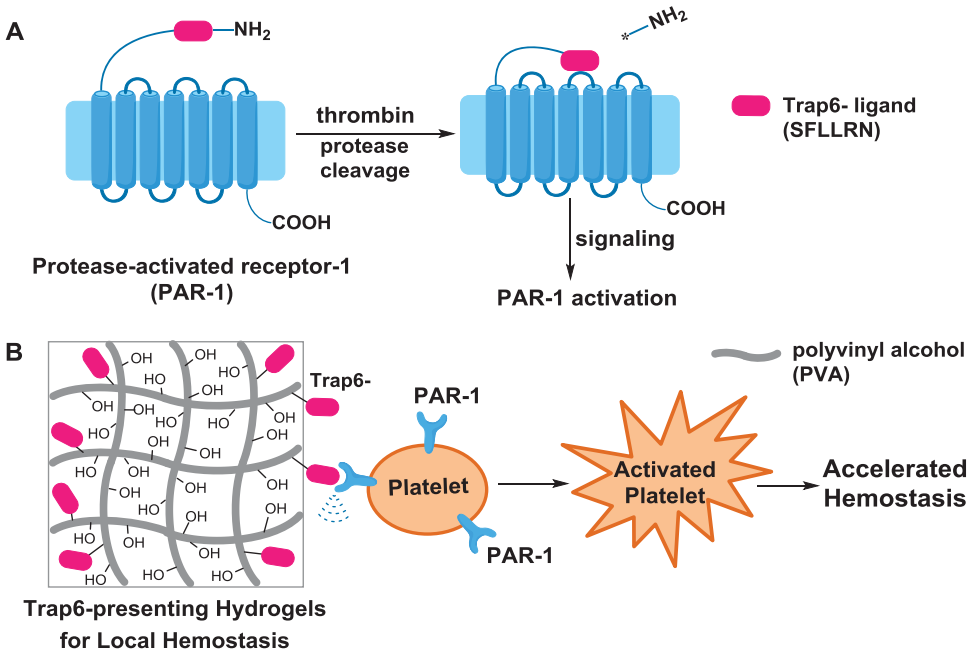

Scheme 1. A) Molecular mechanism of protease-activated receptor-1 (PAR-1) activation. PAR-1 is highly expressed in platelets, and PAR-1 activation is initiated by proteolytic cleavage of part of the extracellular N-terminal domain of the receptor by a serine protease such as thrombin. Proteolysis generates a new N-terminal ligand domain (SFLLRN, a.k.a. thrombin receptor agonist peptide, TRAP6) that interacts with the receptor within the extracellular loop 2 and triggers the signaling pathway of PAR-1 activation. It is known that short TRAP6-derived peptide sequences can also interact with and activate PAR-1.[15] B) TRAP6- peptide motifs are covalently immobilized within synthetic polyvinyl alcohol (PVA) hydrogels, i.e., TRAP6-presenting hydrogels, which are capable of activating platelets in a highly localized manner.

Multiplate TRAP test has become a standard assay in whole blood for quantitative determination of platelet function triggered by TRAP6. Interestingly, TRAP test allows analysis of platelet function activated through PAR-1 signaling without triggering fibrin formation, which otherwise occurs when thrombin is the agonist.

Polyvinyl alcohol (PVA) is a water-soluble polymer originated from partial hydrolysis of polyvinyl acetate. PVA-based hydrogels have been widely used in tissue engineering and drug delivery systems because of their superior biocompatibility (FDA-approved).[16] In addition, PVA hydrogels are well known for being uniquely stronger than most other synthetic hydrogels.

In this work, we demonstrate for the first time that TRAP6 platelet-activating peptide can be covalently immobilized in synthetic hydrogel matrices (Scheme 1B) for hemorrhage control. We tested the hypothesis that polymer-conjugated TRAP6 peptides can maintain their activity for platelet activation while accelerating hemostasis in a safe, localized manner. We designed water-soluble PVA-TRAP6 conjugates as model platelet-activating polymers as well as insoluble (crosslinked) PVA-TRAP6 hydrogel particulates (PVA-TRAP6-P) for safe and localized acceleration of hemostasis. These new polymer–peptide conjugates were prepared using highly efficient thiol-norbornene photoclick chemistry. The extent to which these materials could activate platelets was systematically characterized using rotational thromboelastography (ROTEM), platelet aggregation assay (Multiplate), and flow cytometry (FACS).

2. Results and Discussion

2.1. Materials Design and Synthesis

In this study, a linear synthetic polymer PVA was selected as the substrate for covalent immobilization of the potent platelet-activating peptide (TRAP6) due to the following reasons. First, PVAs are FDA-approved polymers with superior cost-efficacy and cytocompatibility, therefore intriguing for many biomedical applications.[17] Second, the existence of a high number of hydroxyl groups in PVA offers significant freedom for tunable functionalization and presentation of bioactive ligands, which is not available with other synthetic substrates such as arm-dependent polyethylene glycol (PEG).

To introduce TRAP6 peptides onto PVA, we chose the robust thiol-ene photoclick chemistry as the conjugation approach. On one hand, norbornene group was selected as the ene functionality due to its ultrahigh reactivity toward thiol-ene reaction as well as low cytotoxicity.[18,19] On the other hand, we engineered a cysteine moiety with a free thiol group into the C-terminus of a TRAP6 peptide sequence (SFLLRNPNC), since it is accepted that the N-terminus of TRAP6 sequence is critical for its ability to activate platelets.[15]

PVA-NB was synthesized through a facile esterification reaction between PVA and norbornene anhydride for 12 h at 50 °C in DMSO (**Figure 1**A). One notable advantage of this modification approach is that after modification a high number of carboxylate groups could be neutralized into the sodium salt form to provide the products with good water-solubility. The crude

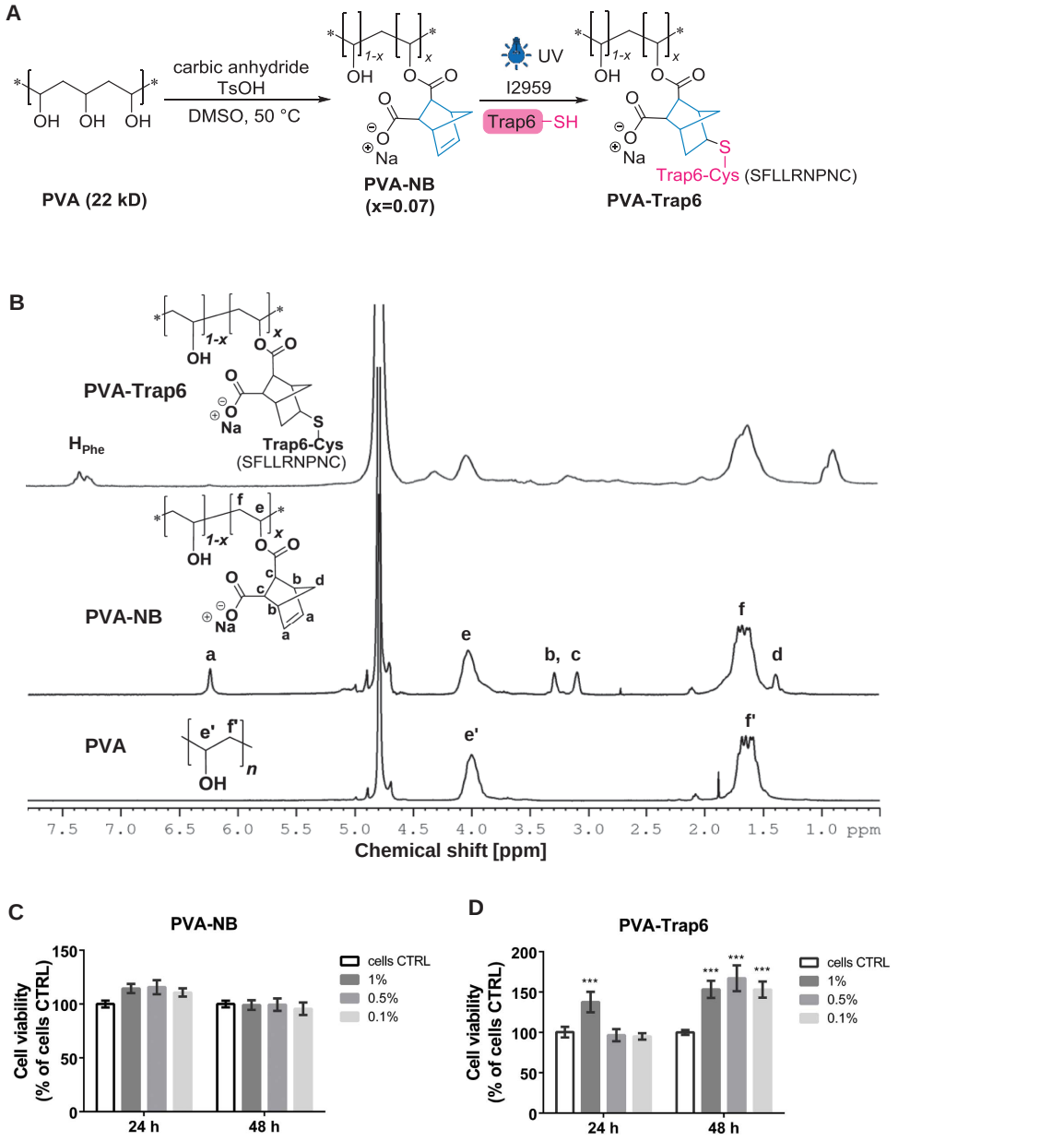

Figure 1. A) Synthesis scheme of PVA-NB (reaction in abs. DMSO at 50 °C for 12 h, TsOH: p-Toluenesulfonic acid) and PVA-TRAP6 (TRAP6-SH: SFLLRNPNC, 1.2 Eq. to NB groups; I2959: Irgacure 2959, i.e., one commonly used water-soluble photoinitiator; 300 s UV irradiation, 20 mW cm^{-2}). B) ^{1}H-NMR (D_2O, 200 MHz) spectra of PVA, PVA-NB, and PVA-TRAP6 conjugate (see integrated spectra in Figure S1, Supporting Information). C,D) normalized viability of C2C12 cells after 24 and 48 h exposure to PVA-NB (C) and PVA-TRAP6 solutions (D) with varying polymer concentrations (1%, 0.5%, and 0.1%) investigated by MTT assay ($n > 3$, "***" indicates $P < 0.001$).

products were purified by sequential dialysis against 10×10^{-3} M $NaHCO_3$ for neutralization and later on against H_2O, and finally lyophilized (>95% yield). To confirm the synthesis, PVA-NB was analyzed using ^{1}H-NMR in comparison with unmodified PVA. As shown in Figure 1B (bottom), the spectrum of unmodified PVA represents two major peaks at 4.0 and 1.6 ppm, which are corresponding to the –CH– and methylene groups, respectively. The spectrum of PVA-NB (Figure 1B, middle) shows new peaks at 6.2 ppm (s, 2H, –CH=CH–), 3.3 ppm (s, 2H, –C=C–CH–CH–), 3.1 ppm (s, 2H, –C=C–CH–CH–), and 1.3 ppm (s, 2H, $–CH_2–$), respectively. The degree of substitution (DS) of PVA-NB was determined (see Figure S1b, Supporting Information) by comparing the integral values corresponding to signals (a, d, f). By changing either the stoichiometry or reaction time, it was feasible to precisely control the DS in a wide range from 5% to 50% (Table S1, Supporting Information). Since PVA (22 kDa) is a linear polymer consisting of ca. 500 repeating units, we selected PVA-NB with the lowest DS (DS-7%) as the precursor, providing ca. 35 reaction sites for photoconjugation with cysteine-containing peptide.

PVA-TRAP6 conjugates (Figure 1A) were prepared by photoconjugation of cysteine-containing TRAP6 peptide with the NB

groups of PVA-NB in PBS solution of I2959 as photoinitiator (PI). To confirm the conjugation efficiency, NMR model reactions were first performed in D_2O. Based on the NMR reaction, Figure 1B (Top) represents the spectrum of PVA-TRAP6 conjugates. The significant decrease of NB proton signals (a) at 6.2 ppm indicates the success of photo-conjugation. Besides, the spectrum of PVA-TRAP6 also shows a new peak at 7.4 ppm, corresponding to the aromatic protons of phenylalanine (Phe or F) moieties in the TRAP6 sequence.

2.2. In Vitro Cytotoxicity

To prove the applicability of the prepared materials for biomedical applications, the in vitro biocompatibility of PVA, PVA-NB, and PVA-TRAP6 solutions was investigated by MTT assay using C2C12 myoblasts. MTT assay showed that PVA (Figure S2, Supporting Information) and PVA-NB (Figure 1C) solutions were nontoxic at varying concentrations (0.1%, 0.5%, 1%) after 24 and 48 h incubation. For the PVA-TRAP6 conjugates, the metabolic activity of C2C12 cells (Figure 1D) after 24 h incubation was significantly increased when mixed with 1% PVA-TRAP6 ($P < 0.001$), while not increased for 0.5% and 0.1% PVA-TRAP6. After 48 h incubation, the metabolic activity for all three concentrations was significantly increased compared to the control ($P < 0.001$). Several studies by other groups have shown that PAR-1 activating peptide such as TRAP6 can stimulate cytokine release from different cell types, including human gingival fibroblasts, endothelial cells, intestinal epithelial cells, and human muscle myoblasts.[20] Therefore, we speculate that the increased metabolic activity of C2C12 myoblasts during MTT assay was attributed to TRAP6-induced PAR-1 activation. Considering that a 1% PVA-TRAP6 solution gives a TRAP6-concentration of 5×10^{-3} M whereas the effective TRAP6-concentration for platelet activation is in the range of 5×10^{-6} to 100×10^{-6} M,[12] the toxicity results suggest that PVA-TRAP6 are cytocompatible materials within its effective range.

2.3. Hemostatic Activity

2.3.1. Thromboelastometry

We next studied the hemostatic efficacy of PVA-TRAP6 in comparison with TRAP6 and PVA-NB using rotational thromboelastometry (ROTEM),[21,22] which is a clinical diagnostic tool allowing in situ characterization of viscoelastic properties of blood clot during coagulation. **Figure 2**A shows the plotted ROTEM curves of the studied samples that were mixed with recalcified whole blood. Clotting time (CT) refers to the latency until the clot reaches a firmness of 2 mm while maximum clot firmness (MCF) refers to the maximum amplitude of the curve, which indicates the absolute strength of the clot.

From the ROTEM results, it was observed that the CT of PVA-TRAP6 at 0.1×10^{-3} M was very comparable to that of TRAP6 at 0.1×10^{-3} M while the MCF of PVA-TRAP6 was relatively less than that of TRAP6 control. The lower MCF is possibily due to the decreased accessibility of TRAP6 to platelets after conjugation in PVA-TRAP6, which is a macromolecular conjugate (ca. 65 kDa) and significantly larger than TRAP6 (ca. 1 kDa). In comparison, the PVA-NB control (Figure 2C) showed a curve very similar to the physiological curve (NaCl control), showing no hemostatic activity of the PVA-NB backbone.

To test whether the hemostatic activity of PVA-TRAP6 is dose-dependent, we tested PVA-TRAP6 solutions in comparison with TRAP6 solutions at three peptide concentrations (0.01×10^{-3}, 0.1×10^{-3}, 1×10^{-3} M) in ROTEM (Figure 2B). It was found that the optimal hemostatic concentration for PVA-TRAP6 was 0.1×10^{-3} M while there was no significant dose influences for TRAP6 control in the chosen range. This may again imply the influence of differential molecular structure in PVA-TRAP6 and TRAP6 peptide on the saturation level of TRAP6 for platelet activation.

2.3.2. Multiplate Analysis

In order to quantify the extent of platelet activation, we utilized Multiplate assay to investigate the influence of PVA-TRAP6, TRAP6, and PVA-NB on platelet aggregation. The principle of this method is based on the fact that platelets become sticky upon activation, and thus prone to adhere and aggregate on the metal sensor wires in the Multiplate test cuvette. As activated platelets adhere and aggregate on the sensor wires, the electrical resistance between the wires rises, which can be continuously monitored. A typical Multiplate curve (Figure 2D) represents the accumulation of electronic signals corresponding to the extent of platelet aggregation. One key parameter of Multiplate assay is aggregation area (in Units), i.e., the area underneath the aggregation curve. It was observed that PVA-TRAP6 (0.1×10^{-3} M) induced an aggregation curve (Figure 2D) that was comparable to that of TRAP6 (0.1×10^{-3} M), while the PVA-NB control displayed negligible capability of platelet aggregation. The aggregation area value (Figure 2E) for TRAP6 was 147 U whereas the area value for PVA-TRAP6 and PVA-NB was 130 U and 2 U ($P < 0.001$), respectively. Together, Multiplate assay proved that PVA-TRAP6 presented high efficiency for platelet activation while the substrate (PVA-NB) did not.

2.3.3. FACS of the Soluble System

We next utilized FACS to quantify the extent of platelet activation. Platelets can be distinguished from other blood cells by the constitutive expression of the surface antigen CD41, which is known as the platelet membrane glycoprotein GpIIb and is noncovalently associated with GpIIIa (the integrin beta 3 chain) to form the GpIIb/IIIa complex. Importantly, the CD62p (P-selectin) membrane glycoprotein is exclusively expressed on activated platelets. The CD62p marker was used to identify the extent of activation in human platelets after incubation with the studied materials (PVA-TRAP6, TRAP6, PVA-NB, and NaCl). The measurement of the CD41/CD62p coexpression (**Figure 3**A–C) in blood samples treated with these materials for 15 min revealed that there was significant effect (ca. 80%) of PVA-TRAP6 (0.1×10^{-3} M) on the CD62p expression in CD41 positive cells. The percentage of activated platelet phenotype in terms of CD62p positive cells stayed

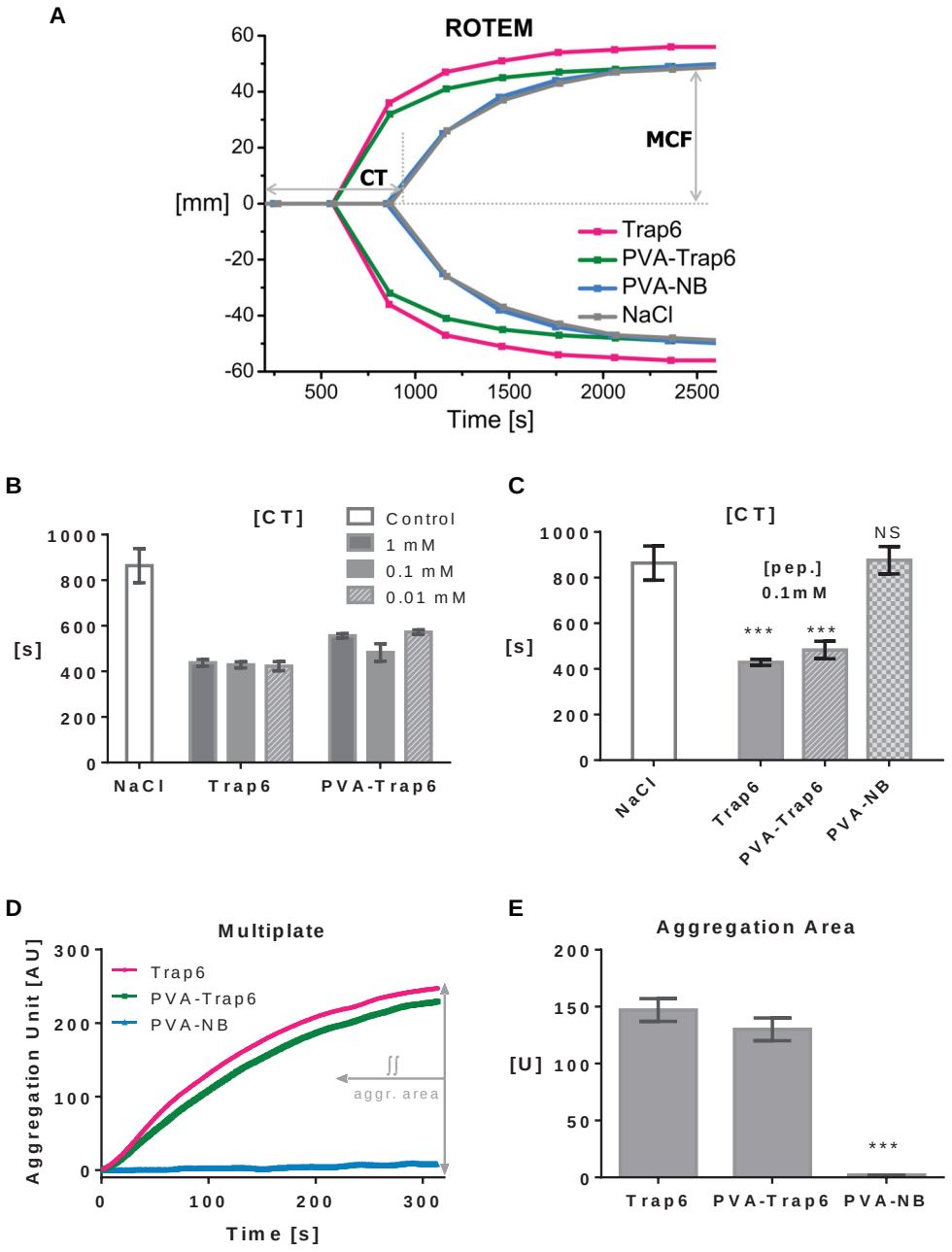

Figure 2. A–C) ROTEM characterization of the coagulation process of whole blood in response to the investigated materials (CT: clotting time in seconds, i.e., the latency until the clot reaches a firmness of 2 mm; MCF: maximum clot firmness in mm). (A) Plotted ROTEM curves showing the coagulation process of whole blood in response to TRAP6 (0.1×10^{-3} M), PVA-TRAP6 (0.1×10^{-3} M TRAP6-), PVA-NB, and 0.9% NaCl control; (B) Influence of unconjugated- and conjugated-TRAP6 (PVA-TRAP6) at varying dosage (0.01, 0.1, 1×10^{-3} M) on CT; and (C) comparative analysis on CT between TRAP6, PVA-TRAP6, and PVA-NB at optimal TRAP6- concentration (0.1×10^{-3} M). D) Multiplate analysis of platelet function in response to TRAP6 (0.1×10^{-3} M), PVA-TRAP6 (0.1×10^{-3} M TRAP6), and PVA-NB; each measurement was performed in duplicate. E) Comparison of the key parameter in Multiplate: aggregation area in Units.

at the same level of the control sample treated with TRAP6 (0.1×10^{-3} M). By contrast, there was no significant effect (<10%) of PVA-NB on the CD62p expression in CD41 positive cells, which was at the same level of the negative control samples treated with 0.9% NaCl. In all, FACS analysis further confirmed the high efficiency of PVA-TRAP6 for platelet activation.

2.4. Preparation and Characterization of PVA Hydrogels

Since platelet-activating PVA-TRAP6 conjugates in soluble form have the potential to cause thrombotic risks in the circulation, we further developed an insoluble PVA-TRAP6 system for localized hemostasis whereby TRAP6 peptide were covalently immobilized in photocrosslinked PVA hydrogel matrices. We

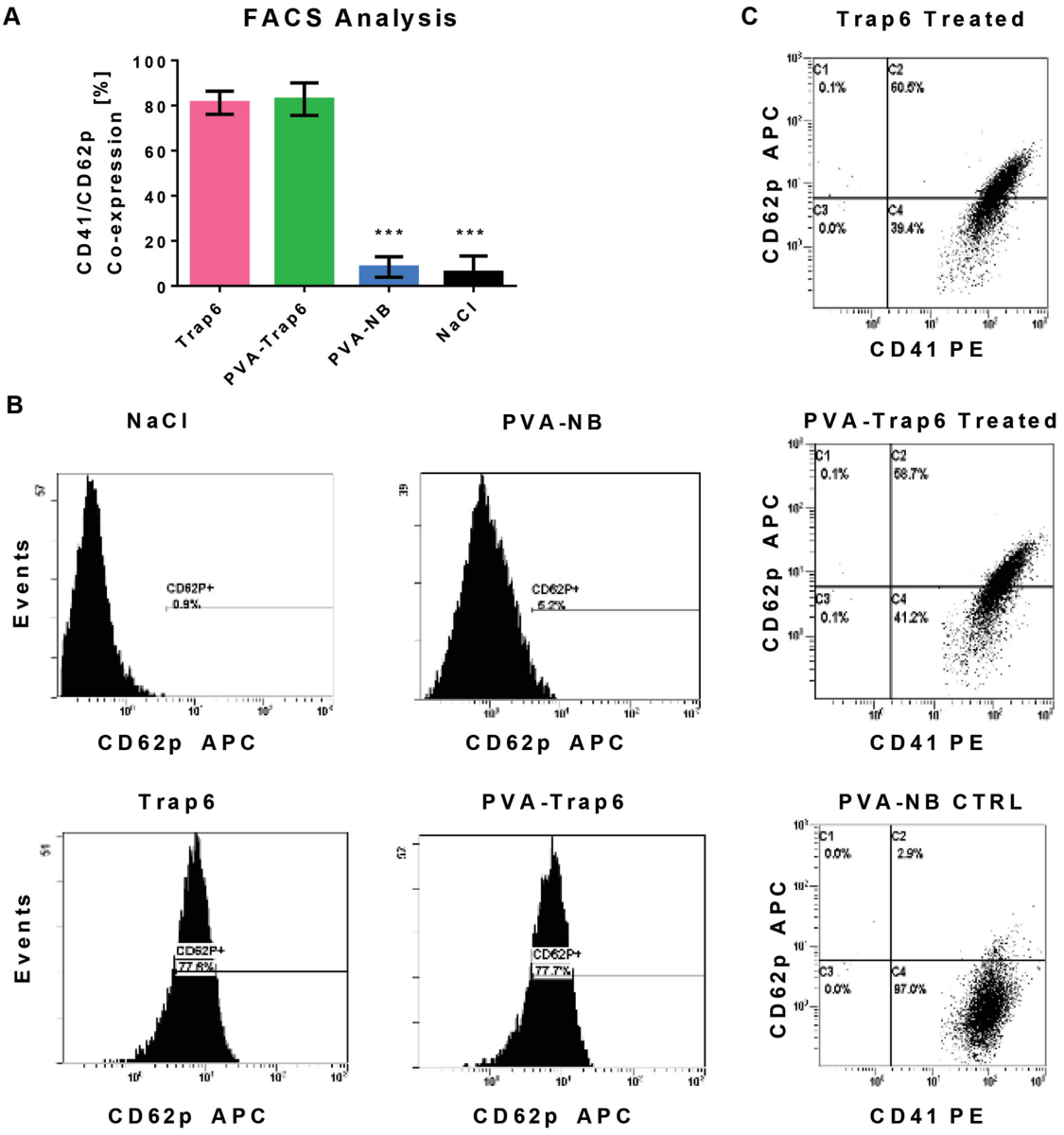

Figure 3. A) FACS analysis of TRAP6-mediated platelet activation measured by determination of CD62p/CD41 coexpression after 15 min incubation. Experiments were run in duplicate, data are presented as percentage of platelets positive for both CD62p and CD41 epitopes ± SD. B) Histogram plots showing the value of the sample stained with the specific CD41 PE and CD62p APC antibodies. C) Representative dot-plots for the expression of CD62p and CD41 of a TRAP6 treated sample, a PVA-TRAP6 treated sample, and a PVA-NB treated control after 15 min incubation.

selected radical-mediated thiol-NB photopolymerization as the approach to create PVA hydrogel matrices (**Figure 4**A). In contrast to conventional crosslinking chemistry of (meth)acrylates, thiol-NB photopolymerization offers several advantages, including robust kinetics, excellent spatiotemporal control, and cytocompatible conditions.[19,23] For instance, PEG-based thiol-NB hydrogels have enabled in situ photoencapsulation of mammalian cells with high level of viability (>90%).[19] In this study, PVA-NB macromers in combination with a model dithiol crosslinker (dithiothreitol, DTT) were photopolymerized under UV irradiation in the presence of I2959 as a water-soluble and biocompatible PI.

2.4.1. Photorheometry

We utilized in situ photorheometry to test the photoreactivity and mechanical properties of PVA hydrogels. It is hypothesized that the chemo-physical properties of PVA hydrogels could be easily adjusted by tuning the thiol to NB ratio. Four PVA-NB/DTT formulations with equal macromer content (10%) but varying thiol to NB ratios (0.4, 0.8, 1.0, 1.2) were screened in photorheometry (Figure 4B). After a 60 s blank period (no UV), upon UV irradiation the storage moduli (G′) of PVA hydrogels increased to different extents (8–120 kPa) in seconds until reaching a G´-plateau. It was found that all of

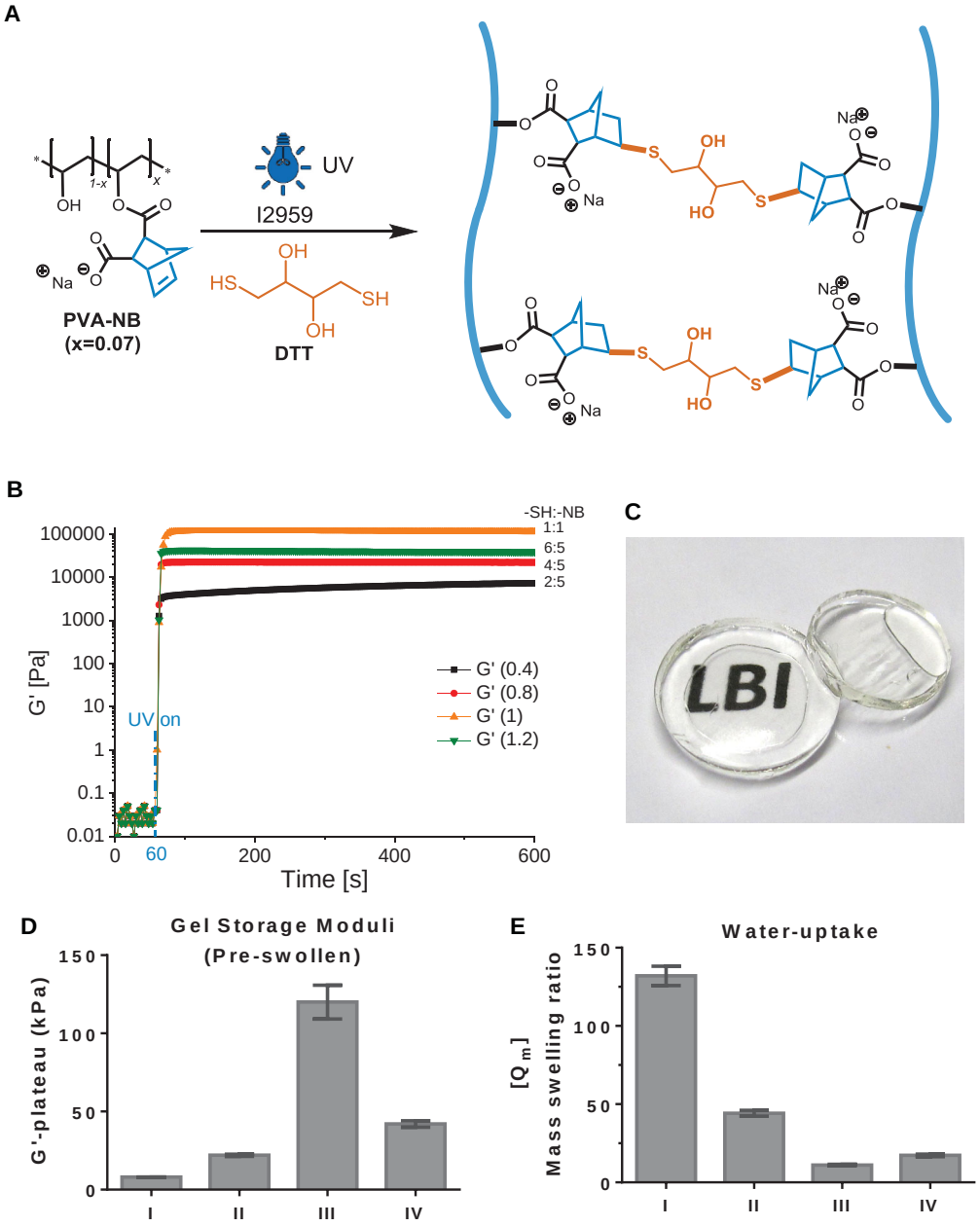

Figure 4. A) Schematic showing the preparation of PVA-NB hydrogels by UV-photocrosslinking of PVA-NB with dithiothreitol (DTT) through radical-mediated photoclick chemistry. B) Mechanical characterization of PVA hydrogels with varying thiol-to-NB ratios (0.4, 0.8, 1.0, and 1.2) using in situ oscillatory photorheometry: G′-gel storage moduli, 10% PVA-NB, 0.5% I2959, 60 s delay, light intensity: 20 mW cm^{-2}; 50 μm gap thickness, 10% strain, 10 Hz. C) Representatives of photopolymerized PVA-NB hydrogel pellets (scale bar: 1 cm). D) Influence of thiol-to-NB ratio (N) on the G′-plateau value: N = 0.4 (I), 0.8 (II), 1.0 (III), 1.2 (IV). E) Equilibrium mass swelling ratios (Q_m) of PVA-NB hydrogels (I–IV) after swelling in PBS for 48 h.

the photopolymerized PVA hydrogels were totally transparent (Figure 4C). By increasing the thiol to NB ratio from 0.4 to 1.2, the G′-plateau values (Figure 4D) changed from 8, 22, 120 to 45 kPa, respectively. The highest G′-plateau value was obtained for hydrogel (III) whereby the thiol to NB ratio was 1:1, indicating the highest degree of crosslinking. Notably, these G′-plateau values from photorheometry measurements can only represent the temporal storage moduli of PVA hydrogels in the preswollen state, as the swelling process could affect the storage moduli of the final materials.[24] Further investigation into the mechanical properties of swollen PVA hydrogels is warranted by using alternative approaches such as AFM nanoindentation.

2.4.2. Water-Uptake

We further analyzed the water-uptake properties of PVA hydrogels (I–IV). Photopolymerized PVA hydrogel pellets were soaked in PBS for 48 h to reach an equilibrium wet weight (m_{wet}), which was compared to the polymer dry weight (m_{dry}) after lyophilization

and give the equilibrium mass swelling ratio (Q_m). As shown in Figure 4E, the Q_m values of hydrogels (I–IV) changed from 130, 45, 10 to 17. In combination with the G′-plateau values, these data suggest that the highest crosslinking degree was obtained when the thiol to NB ratio was 1:1 (III). This observation correlates with previous studies on PEG-based thiol-NB hydrogels by other groups.[19,25] For instance, Shih and Lin demonstrated that thiol-NB photopolymerized PEG hydrogels are hydrolytically degradable due to the presence of ester bonds.[25] The degradation rate was dependent on the gel crosslinking density, which was dictated by thiol to NB ratio and macromer content. Since presented PVA hydrogels also possess a number of ester linkages, we anticipate that these hydrogels are hydrolytically degradable. Besides DTT, alternative di-cysteine protease-sensitive peptides can also be used as enzymatically cleavable crosslinker[26] in order to foster cellular remodeling and wound healing. Nevertheless, further investigation into the degradation behavior of presented PVA hydrogels in vitro and in vivo is needed.

2.5. Biofunctionalization

2.5.1. Preparation of TRAP6-Functionalized Hydrogel Particulates

In order to prepare appropriate hydrogel matrices for TRAP6-functionalization, photopolymerized PVA hydrogels (I, -SH:-NB = 0.4) were sequentially lyophilized and cryo-milled into fine particulates (**Figure 5**A). Since excessive NB groups were present

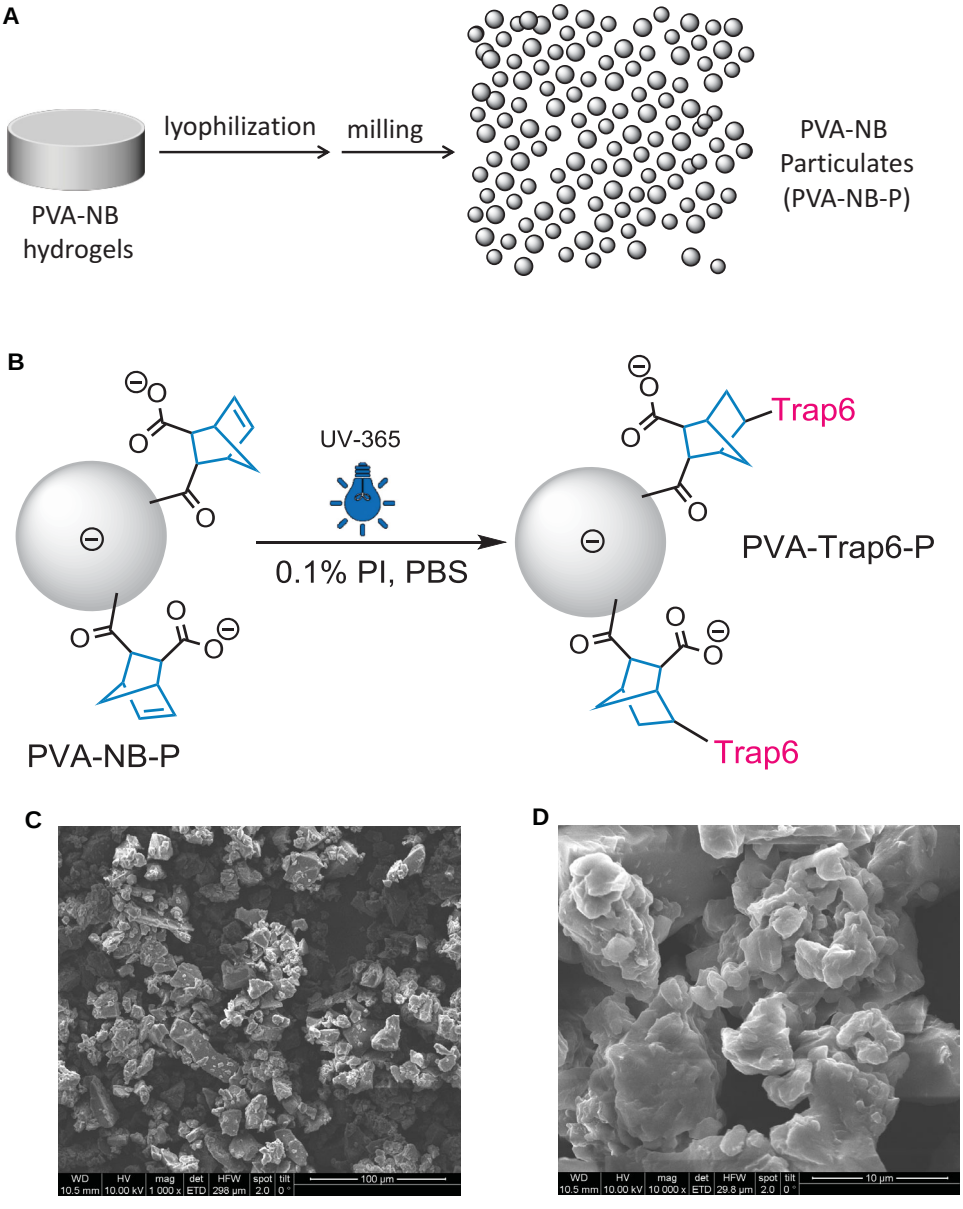

Figure 5. A) Schematics of the preparation of PVA hydrogel (I, -SH:-NB = 0.4) particulates (PVA-NB-P) by sequential lyophilization and cryo-milling; B) schematics of the surface functionalization of PVA-NB-P with cysteine-containing TRAP6 peptide via light-triggered thiol-NB conjugation, -SH:-NB = 1.2, 0.1% PI (LAP) in PBS, 20 mW cm^{-2}; C,D) SEM images of PVA-TRAP6-P, scale bars: (C) 100 µm, (D) 10 µm.

after photopolymerization, these residual groups were exploited for photoclick conjugation (Figure 5B) with cysteine-containing TRAP6 peptide. SEM analysis (Figure 5C) revealed that the length scale of PVA-TRAP6-P was in the range of 5–50 μm. The partial agglomeration of PVA-TRAP6-P was presumably due to the charge effects of NB groups.

2.5.2. ROTEM Analysis

We tested the hemostatic ability of PVA-TRAP6-P in comparison with PVA-NB-P in ROTEM. Prior to test, these particulates were carefully mixed with saline to form injectable slurries. As shown in **Figure 6**A,B, the addition of PVA-TRAP6-P into whole blood induced a significant decrease of CT to ca. 50% of the physiological CT. Interestingly, the PVA-NB-P control also induced a decrease of CT to ca. 70%. Since negatively charged surfaces are known to contribute to the coagulation cascade (i.e., the intrinsic pathway),[27] we suppose that the observed hemostatic activity of PVA-NB-P is due to the charge effects of NB groups.

2.5.3. FACS Analysis

In order to quantify the ability of these particulated materials to activate platelets, we analyzed whole blood samples that were preincubated with PVA-TRAP6-P and/or PVA-NB-P in FACS. FACS analysis (Figure 6C–F) revealed that the percentage of activated platelets ($CD41^+/CD62p^+$) for PVA-TRAP6-P was as high as ca. 55%, which was comparable to the positive control (0.1×10^{-3} M TRAP6). By contrast, blood samples incubated with PVA-NB-P only exhibited a minimal amount of activated platelets (<10%). These results show that TRAP6-presenting hydrogel matrices (PVA-TRAP6-P) present good potency of activating platelets in a localized manner. Furthermore, these data imply that the hemostatic activity of PVA-NB-P was not due to platelet activation, but instead other factors such as providing a catalytic surface that accelerates coagulation via intrinsic pathway.

3. Conclusion

In this work, we developed a synthetic hemostatic hydrogel system that can efficiently activate platelets and accelerate hemostasis in a localized manner. The use of highly potent protease, thrombin, is avoided in this system. Instead, the thrombin-receptor-agonist-peptide-6 (TRAP6) was covalently engineered on cytocompatible PVA hydrogels via highly efficient thiol-norbornene photoconjugation. The presented TRAP6-functionalization approach is also applicable to other synthetic hydrogels such as PEG as well as naturally derived hydrogels such as gelatin and hyaluronic acid. From a biological point of view, activated platelets are known to release platelet-derived growth factors (PDGF), which regulate cell proliferation and play a significant role in blood vessel formation (angiogenesis). Therefore, we anticipate that these platelet-activating hydrogel matrices are versatile biomaterials not only for safe hemostasis but also for potential applications in tissue regeneration and wound healing.

4. Experimental Section

Materials and Reagents: All reagents were purchased from Sigma-Aldrich and used as received unless otherwise noted.

Synthesis of PVA-Norbornene (PVA-NB): In a three-neck flask, PVA (10 g) and p-toluenesulfonic acid (20 mg) were dissolved in anhydrous DMSO (250 mL) at 60 °C for 1 h under argon atmosphere. In a second flask, under argon atmosphere *cis*-5-norbornene-endo-2,3-dicarboxylic anhydride (2 g, 0.1 eq. to –OH groups) was dissolved in anhydrous DMSO (50 mL). The obtained solution was added dropwise into the first flask containing PVA. The reaction was maintained at 50 °C for 12 h. After reaction, the crude product was purified by dialysis against 10×10^{-3} M $NaHCO_3$ solution for 24 h and subsequently against deionized (DI) water for 12 h. After lyophilization, PVA-NB was obtained as colorless solid in 95% yield. ^{1}H-NMR (D_2O, 200 MHz): δ (ppm): 6.2 (2H, s, –CH=CH–), 3.3 (2H, s, –C=CCH–CH–), 3.1 (2H, s, –C=C–CH–CH–), 1.3 (2H, s, –CH2–). Degree of substitution (DS): 7%.

Synthesis of PVA-TRAP6 Conjugates: PVA-TRAP6 was prepared by covalent attachment of a cysteine-containing TRAP6 peptide (N-C: SFLLRNPNC, China Peptide Co.) onto the backbone of PVA-NB through thiol-ene photoclick conjugation. Specifically, 60 mg of PVA-NB (DS-7%) was dissolved in PBS solution of 0.5% Irgacure 2959 (I2959, BASF) to give a final macromer concentration of 5%. To this solution, TRAP6 peptide (100 mg, 1.2 eq. to NB groups) was added. The obtained solution was stirred under argon and irradiated with filtered UV-light (320–500 nm) for 300 s at 20 mW cm^{-2}. The UV-light was guided from an Omnicure S2000 lamp.

Preparation of PVA-NB Hydrogels: PVA-NB (DS-7%) was dissolved in 0.5% I2959 solution, achieving a final concentration 10%. Then, aliquots of this solution was mixed with appropriate amount of dithiothreitol (DTT), providing –SH/-NB ratios as 0.4 (I), 0.8 (II), 1.0 (III), and 1.2 (IV), respectively. Hydrogel pellets were prepared by photopolymerization in a multi-well PDMS mold (well diameter: 6 mm). Specifically, macromer solutions (200 μL) were pipetted between two glass coverslips separated by the PDMS mold (thickness: 1.5 mm) and then exposed to filtered UV light (20 mW cm^{-2}) for 600 s. The hydrogel pellets were detached from the slides and washed with sterile PBS.

Preparation of PVA-NB Hydrogel Particulates (PVA-NB-P): Hydrogel precursor solutions (I) were prepared as aforementioned and photopolymerized at same conditions except using a 10 mL cylindrical glass vial as the mold. After photopolymerization, the hydrogel cylinders were transferred into a 100 mL beaker and washed with PBS (two changes) for 12 h in order to remove unreacted polymer and PI. Afterward, the swollen hydrogels were frozen with liquid N_2 and lyophilized. Finally, the dry PVA-NB matrix was grinded into fine powders using a RETSCH Cryomill RS232.

Preparation of TRAP6-Presenting PVA Hydrogel Particulates (PVA-TRAP6-P): PVA-TRAP6-P was prepared by covalent attachment of TRAP6 peptide onto the residual NB groups on PVA-NB-P. Specifically, PVA-NB-P (100 mg) was dispersed in PBS solution of 0.1% long-wavelength PI (LAP)[19] to give a final polymer content of 5%. To this suspension, specific amounts of TRAP6 peptide (1.2 eq. to NB groups) were added. The obtained suspension was stirred under argon and irradiated with UV-light (365 nm) for 300 s at 20 mW cm^{-2}. The UV-light (365 nm) was guided from an Omnicure LX400 LED lamp.

Photorheometry: Photorheometry was performed on a modular photorheometer (Anton Paar MCR-302) as previously reported.[28] Specifically, MCR302 was integrated with filtered UV-light (320–500 nm) from a light guide (Omnicure S2000) to the bottom of the glass plate. Plate-to-plate oscillatory photorheometry was applied for real-time monitoring of the curing kinetics of hydrogel formulations during photopolymerization. Light intensity at the plate surface was ca. 20 mW cm^{-2} as determined by an Ocean Optics USB 2000+

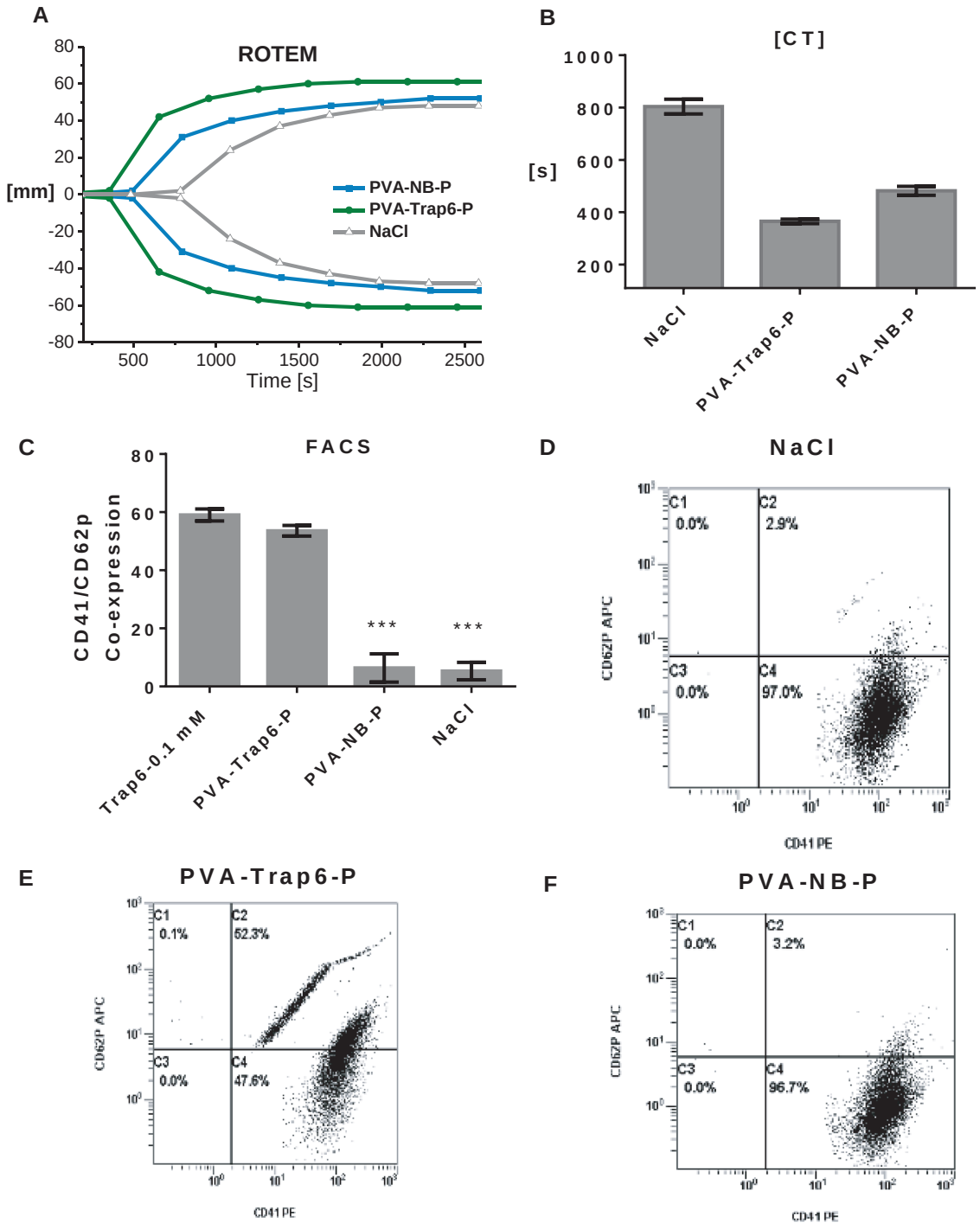

Figure 6. A,B) ROTEM characterization of the coagulation process of whole blood in response to the suspension of PVA-NB-P and PVA-TRAP6-P (10 wt% in saline). A) Plotted ROTEM curves showing the coagulation process of whole blood in response to PVA-NB-P and PVA-TRAP6-P suspensions; B) comparative analysis on the CT between PVA-NB-P, PVA-TRAP6, and NaCl (control). C–F) FACS analysis of particulated polymers. C) FACS analysis of TRAP6-mediated platelet activation measured by determination of CD62p/CD41 coexpression after 15 min incubation. Experiments were repeated twice using blood samples from different donors ($n = 2$), and data are presented as percentage of platelets positive for both CD62p and CD41 epitopes ± SD. (D,E,F) Representative dot-plots for the coexpression of CD62p and CD41 of a PVA-NB-P treated sample and a PVA-TRAP6-P treated sample (positive control: 0.1×10^{-3} M TRAP6, negative control: NaCl) after 15 min incubation.

spectrometer. Both storage moduli (G′) and loss moduli (G″) of the samples could be monitored as a function of irradiation time.

Water-Uptake: Equilibrium mass swelling ratios of PVA-NB hydrogels were tested using a generic protocol.[29] Hydrogel pellets ($n = 3$) were prepared as aforementioned and allowed to swell in PBS for 24 h at room temperature. The wet pellets were weighed to determine the equilibrium wet mass (M_{wet}) and then lyophilized to obtain the dry weight (M_d). The equilibrium mass swelling ratio (Q_m) was calculated as M_{wet}/M_d.

MTT Assay: Cytotoxicities of PVA, PVA-NB, and PVA-TRAP6 macromer solutions were evaluated via MTT assay. C2C12 cells were cultured in Dulbecco's modified eagles medium (DMEM) supplemented with 5% fetal calf serum (FCS), 1% L-glutamine, 1% penicillin/streptomycin. Macromer solutions with three concentrations (5%, 1%, and 0.1%) were prepared in DMEM solutions. C2C12 cells were then seeded in a 96-well plate at a density of 5×10^3 cells per well in 200 µL of culture medium. After 24 h incubation (37 °C, 5% CO_2), 100 µL of the respective macromer solutions were added to the cells in triplicates. After 24 h incubation, cells were washed twice with sterile PBS before the addition of 100 µL thiazolyl blue tetrazolium bromide (MTT) working solution (5 mg mL^{-1} in PBS). After 1 h incubation, the liquid was discarded and 100 µL of DMSO was added to dissolve the formazan crystals. Finally, the absorbance was measured at 540 nm using a microplate reader.

Rotational Thromboelastometry: ROTEM (TEM Innovation, Germany) was applied to monitor the interactions of platelet-activating polymers and whole blood over time. ROTEM system contains an oscillating sensor pin that is immersed in a temperature-controlled cuvette containing the blood sample. Four measurements can be performed in parallel in the same device. Generally, coagulation of the citrated blood sample is initiated by recalcification. The formation kinetics of a fibrin clot could be monitored mechanically and calculated by an integrated computer to the typical curves and numerical parameters.

Blood was collected from three unmedicated and healthy donors using minimal stasis from an antecubital vein through a 21-gauge needle. The use of human blood was approved by the Ethical Commission of the Austrian Social Insurance for Occupational Risks (AUVA) Center for Traumatology Research. After discarding the first 3 mL, blood was collected in 3.5 mL tubes (Vacuette; Greiner Bio-One) containing 0.3 mL buffered 3.2% sodium citrate. The samples were kept on a prewarming stage at 37 °C for at least 10 min prior to analysis and were processed within 3 h. ROTEM analysis of the whole blood sample was initiated by recalcification with the addition of 20 µL of $CaCl_2$ (star-TEM, 200×10^{-3} M). Polymer solutions and/or polymer suspensions were added directly to the cuvette immediately after recalcification of the citrated blood and mixed by gently pipetting up and down as previously reported.[21] The final reaction volume per ROTEM cuvette was 370 µL, consisting of 300 µL citrated whole blood, 20 µL $CaCl_2$ and 50 µL polymer solution or polymer suspension.

The following ROTEM parameters were calculated from the signal and included in the statistical analysis: CT in seconds (s), i.e., the latency until the clot reaches a firmness of 2 mm, which is a measure of initial fibrin formation; clot formation time (CFT) in second, i.e., the time from CT until the clot reaches a firmness of 20 mm, which indicates platelet function and fibrinogen quality; α-angle, the angle (°) between the *x*-axis and the tangent of the forming curve starting from CT point, which is comparable to CFT; MCF in mm, the maximum amplitude of the curve, which indicates the absolute strength of the clot; and A30 (mm), i.e., the clot firmness after 30 min.

Multiplate Analysis: The principle of Multiplate test is based on the fact that platelets become sticky upon activation, and thus prone to adhere and aggregate on the metal sensor wires in the Multiplate test cuvette. The sensor wires are made of highly conductive copper, which is silver-coated. As activated platelets adhere and aggregate on the sensor wires, the electrical resistance between the wires rises, which could be monitored in real time. For each measurement, 300 µL of saline and 300 µL of hirudinized whole blood was added sequentially to a Multiplate cuvette. After 3 min incubation at 37 °C, 20 µL of sample solution was added and at the same time the program started to collect signals. The Multiplate device allows four measurements in parallel. Each measurement was performed for 6 min and in duplicate.

FACS Analysis: Citrated whole blood (WB) from two healthy donors was diluted in 1:10 (v/v) with a modified HEPES-Tyrode's buffer (HT-Buffer: 10×10^{-3} M HEPES, 137×10^{-3} M NaCl, 2.8×10^{-3} M KCl, 1×10^{-3} M $MgCl_2$, 12×10^{-3} M $NaHCO_3$, 0.4×10^{-3} M Na_2HPO_4, 0.35% BSA, 5.5×10^{-3} M glucose). To 15 µl of diluted WB, 70 µl of HT-Buffer as well as 5 µl of CD41a-PE and 5µl of CD62P-APC (pre-diluted in 1:4 with HT-Buffer) were added. After an incubation of 20 min at room temperature under light protection, 20 µl of PVA-TRAP6 solution (3 mg mL^{-1} in saline to obtain a final TRAP6 concentration of 0.2×10^{-3} M) were added and platelets were stimulated for 15 min. Twenty microliter of TRAP6 solution (14 mg mL^{-1}) and 20 µL of NaCl solution (0.9%) were added as the positive control and the negative control, respectively. The samples were fixed with 300 µl of formalin (1%) for 15 min at room temperature, subsequently tested on a Beckman Coulter FC 500 MPL flow cytometer (Germany), and finally analyzed with CXP software. A threshold was set on CD41a to identify the platelet population and combined with the plot of log forward scatter (FSC) and side scatter (SC).

SEM: The lyophilized hydrogel particulates were mounted on stubs, sputter-coated with Pd/Au and finally analyzed on a scanning electron microscope (FEI Quanta 200).

Statistics: All error bars indicate the standard deviation. The statistical significance was determined by student's t-test, where "*", "**", "***" indicate $P < 0.05$, $P < 0.01$, $P < 0.001$, respectively.

Supporting Information

Supporting Information is available from the Wiley Online Library or from the corresponding author (Dr. X.-H. Qin).

Acknowledgements

We would like to thank Stephan Benedikt for the synthesis of water-soluble long-wavelength photoinitiator, Daniel Bomze for the help with precursor synthesis, Anton Klotz for the FACS test assays, Elisabeth Eitenberger for the SEM imaging and Sylvia Nürnberger for the attempts of clot histological analysis. In addition, we like to thank Andreas Gössl, Christoph Schlimp and Johannes Zipperle for fruitful scientific discussions. This work is supported by the Headquarter program (H.R.) of the Austrian Research Promotion Agency (FFG) and the Precision Polymer Materials Network (R.L.) of the European Science Foundation (ESF-P2M).

Received: April 22, 2015
Revised: May 28, 2015
Published online: October 6, 2015

[1] H. B. Alam, D. Burris, J. A. DaCorta, P. Rhee, *Mil. Med.* **2005**, *170*, 63.
[2] a) W. D. Spotnitz, S. Burks, *Transfusion* **2008**, *48*, 1502; b) A. M. Behrens, M. J. Sikorski, P. Kofinas, *J. Biomed. Mater. Res., Part A* **2014**, *102*, 4182.
[3] a) H. Redl, G. Schlag, in *Fibrin Sealant in Operative Medicine* (Eds: G. Schlag, H. Redl), Springer, Berlin **1986**, p. 13; b) H. C. Hedrich, M. Simunek, S. Reisinger, J. Ferguson, H. Gulle, A. Goppelt, H. Redl, *J. Biomed. Mater. Res., Part B* **2012**, *100B*, 1507.
[4] a) T. A. Ostomel, Q. Shi, G. D. Stucky, *J. Am. Chem. Soc.* **2006**, *128*, 8384; b) T. A. Ostomel, Q. Shi, P. K. Stoimenov, G. D. Stucky, *Langmuir* **2007**, *23*, 11233.
[5] a) M. C. Oz, J. F. Rondinone, N. S. Shargill, *J. Card. Surg.* **2003**, *18*, 486; b) L. Y. Han, V. Schimp, J. C. Oh, P. T. Ramirez, *Int. J. Gynecol. Cancer* **2004**, *14*, 621; c) R. Lemmer, M. Albrech, G. Bauer, *J. Obstet. Gynaecol. Res.* **2012**, *38*, 435.
[6] M. Mehdizadeh, J. Yang, *Macromol. Biosci.* **2013**, *13*, 271.
[7] T. J. Guzzo, R. A. Pollock, A. Forney, P. Aggarwal, B. R. Matlaga, M. E. Allaf, *J. Endourol.* **2009**, *23*, 279.
[8] A. Gugerell, K. Schossleitner, S. Wolbank, S. Nürnberger, H. Redl, H. Gulle, A. Goppelt, M. Bittner, W. Pasteiner, *J. Biomed. Mater. Res., Part A* **2012**, *100A*, 1239.

[9] a) H. H. Versteeg, J. W. M. Heemskerk, M. Levi, P. H. Reitsma, *Physiol. Rev.* **2013**, *93*, 327; b) S. R. Coughlin, *Nature* **2000**, *407*, 258.
[10] H. P. Kohler, *Blood* **2013**, *121*, 1931.
[11] K. J. Clemetson, *Thromb. Res.* **2012**, *129*, 220.
[12] S. R. Macfarlane, M. J. Seatter, T. Kanke, G. D. Hunter, R. Plevin, *Pharmacol. Rev.* **2001**, *53*, 245.
[13] H. Andersen, D. L. Greenberg, K. Fujikawa, W. Xu, D. W. Chung, E. W. Davie, *Proc. Natl. Acad. Sci. U. S. A.* **1999**, *96*, 11189.
[14] a) S. R. Coughlin, *J. Thromb. Haemostasis* **2005**, *3*, 1800; b) K. M. Austin, L. Covic, A. Kuliopulos, *Blood* **2013**, *121*, 431.
[15] R. R. Vassallo Jr., T. Kieber-Emmons, K. Cichowski, L. F. Brass, *J. Biol. Chem.* **1992**, *267*, 6081.
[16] a) B. V. Slaughter, S. S. Khurshid, O. Z. Fisher, A. Khademhosseini, N. A. Peppas, *Adv. Mater.* **2009**, *21*, 3307; b) N. A. Peppas, J. Z. Hilt, A. Khademhosseini, R. Langer, *Adv. Mater.* **2006**, *18*, 1345.
[17] R. H. Schmedlen, K. S. Masters, J. L. West, *Biomaterials* **2002**, *23*, 4325.
[18] a) C. E. Hoyle, C. N. Bowman, *Angew. Chem.* **2010**, *49*, 1540; b) C. C. Lin, A. Raza, H. Shih, *Biomaterials* **2011**, *32*, 9685.
[19] B. D. Fairbanks, M. P. Schwartz, A. E. Halevi, C. R. Nuttelman, C. N. Bowman, K. S. Anseth, *Adv. Mater.* **2009**, *21*, 5005.
[20] a) L. Hou, S. Ravenall, M. G. Macey, P. Harrlott, S. Kapas, G. L. Howells, *J. Periodontal Res.* **1998**, *33*, 205; b) N. Asokananthan, P. T. Graham, J. Fink, D. A. Knight, A. J. Bakker, A. S. McWilliam, P. J. Thompson, G. A. Stewart, *J. Immunol.* **2002**, *168*, 3577; c) C. Keller, Y. Hellsten, A. Steensberg, B. K. Pedersen, *Cytokine* **2006**, *36*, 141.
[21] J. Zipperle, C. J. Schlimp, W. Holnthoner, A. M. Husa, S. Nurnberger, H. Redl, H. Schochl, *Thromb. Haemostasis* **2013**, *109*, 869.
[22] H. Schöchl, C. Solomon, V. Laux, S. Heitmeier, S. Bahrami, H. Redl, *Thromb. Res.* **2012**, *130*, e107.
[23] a) X.-H. Qin, A. Ovsianikov, J. Stampfl, R. Liska, *BioNanoMater.* **2014**, *15*, 49; b) J. Torgersen, X.-H. Qin, Z. Li, A. Ovsianikov, R. Liska, J. Stampfl, *Adv. Funct. Mater.* **2013**, *23*, 4542.
[24] A. M. Kloxin, C. J. Kloxin, C. N. Bowman, K. S. Anseth, *Adv. Mater.* **2010**, *22*, 3484.
[25] H. Shih, C. C. Lin, *Biomacromolecules* **2012**, *13*, 2003.
[26] M. P. Lutolf, J. L. Lauer-Fields, H. G. Schmoekel, A. T. Metters, F. E. Weber, G. B. Fields, J. A. Hubbell, *Proc. Natl. Acad. Sci. U.S.A.* **2003**, *100*, 5413.
[27] N. Boknas, L. Faxalv, T. L. Lindahl, S. Ramstrom, *J. Thromb. Haemostasis* **2014**, *12*, 515.
[28] X.-H. Qin, J. Torgersen, R. Saf, S. Muhleder, N. Pucher, S. C. Ligon, W. Holnthoner, H. Redl, A. Ovsianikov, J. Stampfl, R. Liska, *J. Polym. Sci., Pol. Chem.* **2013**, *51*, 4799.
[29] X.-H. Qin, P. Gruber, M. Markovic, B. Plochberger, E. Klotzsch, J. Stampfl, A. Ovsianikov, R. Liska, *Polym. Chem.* **2014**, *5*, 6523.